
Generative Large Language Models Trained for Detecting Errors in Radiology Reports

Cong Sun^{1,†}, Kurt Teichman^{2,†}, Yiliang Zhou¹, Brian Critelli², David Nauheim², Graham Keir², Xindi Wang², Judy Zhong¹, Adam E Flanders³, George Shih^{2,*}, Yifan Peng^{1,*}

¹Department of Population Health Science, Weill Cornell Medicine, New York, NY

²Department of Radiology, Weill Cornell Medicine, New York, NY

³Department of Radiology, Thomas Jefferson University, Philadelphia, PA

*Corresponding author(s). Email(s): ges9006@med.cornell.edu, yip4002@med.cornell.edu

[†]These authors contributed equally to this work.

Abstract

Background: Large language models (LLMs) offer promising solutions, yet their application in medical proofreading, particularly in detecting errors within radiology reports, remains underexplored.

Purpose: To develop and evaluate generative LLMs for detecting errors in radiology reports during medical proofreading.

Materials and Methods: In this retrospective study, a dataset was constructed with two parts. The first part included 1,656 synthetic chest radiology reports generated by GPT-4 using specified prompts, with 828 being error-free synthetic reports and 828 containing errors. The second part included 614 reports: 307 error-free reports between 2011 and 2016 from the MIMIC-CXR database and 307 corresponding synthetic reports with errors generated by GPT-4 on the basis of these MIMIC-CXR reports and specified prompts. All errors were categorized into four types: negation, left/right, interval change, and transcription errors. Then, several models, including Llama-3, GPT-4, and BiomedBERT, were refined using zero-shot prompting, few-shot prompting, or fine-tuning strategies. Finally, the performance of these models was evaluated using the F1 score, 95% confidence interval (CI) and paired-sample t-tests on our constructed dataset, with the prediction results further assessed by radiologists.

Results: Using zero-shot prompting, the fine-tuned Llama-3-70B-Instruct model achieved the best performance with the following F1 scores: 0.769 (95% CI, 0.757-0.771) for negation errors, 0.772 (95% CI, 0.762-0.780) for left/right errors, 0.750 (95% CI, 0.736-0.763) for interval change errors, 0.828 (95% CI, 0.822-0.832) for transcription errors, and 0.780 overall. In the real-world evaluation phase, two radiologists reviewed 200 randomly selected reports output by the model (50 for each error type). Of these, 99 were confirmed to contain errors detected by the models by both radiologists, and 163 were confirmed to contain model-detected errors by at least one radiologist.

Conclusion: Generative LLMs, fine-tuned on synthetic and MIMIC-CXR radiology reports, greatly enhanced error detection in radiology reports.

1 Introduction

Chest radiography is essential for diagnosing thoracic conditions [1, 2]. However, the accuracy of radiology reports can be compromised by several factors. For example, while the speech recognition software commonly used in radiology dictation efficiently transcribe spoken words, they are prone to errors, particularly when dealing with complex radiology terminology or background noise [3–6]. Additionally, further errors can be introduced into radiology reports by variability in perceptual and interpretive processes, as well as cognitive biases [7, 8].

These challenges collectively contribute to frequent errors in radiology reports, ranging from minor discrepancies to clinically significant mistakes [9]. The need for accurate radiology reports cannot be overstated, as even minor errors in these reports can result in severe consequences, such as incorrect diagnoses or delayed treatments [10].

Efforts to reduce radiology report errors have traditionally focused on generating more structured reports [11–14]. However, their adoption among radiologists varies, mainly because of the rigidity of structured reports. In addition to implementing structured reports, the use of deep learning methods [15–20] has proven to be highly effective for detecting errors in radiology reports. While promising, these deep learning methods require substantial amounts of annotated data for training and typically focus on detecting errors at the sentence level.

Recent advancements in large language models (LLMs) provide new opportunities to address these limitations [21–23]. While LLMs have shown potential in radiology applications [24–26], studies evaluating their effectiveness in detecting errors in radiology reports are lacking. Additionally, proprietary LLMs (e.g., ChatGPT) have significant accessibility and implementation challenges, including high costs, data privacy concerns, and regulatory compliance issues [23].

Although a few studies have explored the use of existing LLMs, such as GPT-4, for detecting errors in radiology reports [27, 28], research on evaluating the performance of radiology-specific fine-tuned LLMs for proofreading errors remains in its early stages. For example, Gertz et al. focused on evaluating the potential of GPT-4 for error detection in radiology reports but did not compare its performance with that of other LLMs, particularly those that are locally fine-tuned [27]. Schmidt et al. evaluated five different LLMs, but their analysis was limited to detecting speech recognition errors in radiology reports and did not explore how fine-tuning affects LLM performance. Consequently, critical questions about model optimization and generalization remain unanswered [28].

To bridge these gaps, this study introduces fine-tuned LLMs and evaluates the potential of fine-tuned LLMs for detecting errors in radiology reports during medical proofreading.

2 Materials and Methods

This study utilized deidentified data and publicly available LLMs; therefore, it did not require an Institutional Review Board (IRB) review.

2.1 Dataset Construction

The constructed dataset consists of two parts (Table 1). The first part contained synthetic radiology reports generated by GPT-4-0125-Preview using specified prompts (Figure 1). This process involved carefully crafting prompts and providing detailed instructions to guide GPT-4-0125-Preview in generating relevant radiology reports. Once the prompt was input into GPT-4-0125-Preview, the model processed the information and generated synthetic radiology reports accordingly (Figure 1).

In this study, four types of errors frequently encountered in radiology reports were considered: negation,

<p><Report Template> CLINICAL HISTORY: [] TECHNIQUE: AP chest and abdomen radiograph. [] COMPARISON: [Radiograph from one day prior]. FINDINGS: Lines/tubes: [None] Mediastinum/Heart: The cardiomeastinal silhouette is [unremarkable.] Lungs/Airways/Pleura: [No focal opacities, pneumothorax or pleural effusion.] Bones/Soft Tissue: [No acute osseous abnormalities.] Upper abdomen: [Unremarkable] IMPRESSION: [] </Report Template></p> <p>You are a radiologist assistant helping to create synthetic reports using the <Report Template> above.</p> <p>Please follow instructions carefully, and only output what is expected below and nothing more.</p> <p>Radiology reports can have a variety of errors and issues. 'Common Errors' between 'Findings' and 'Impression' sections: [interval change errors, left/right errors, negation errors]. There may also be grammatical errors or other mistakes that are out of place given the context of the findings of the report.</p> <p>Left/right error examples: - [Findings] Possible right upper lobe consolidation. [Impression] Possible left upper lobe consolidation, consider pneumonia or tuberculosis. - [Findings] Possible rib fracture on the right. [Impression] Possible left-sided rib fracture.</p> <p>Interval change error examples: - [Findings] Lungs/Airways/Pleura: Unilateral lower lobe consolidation, consistent with pneumonia. [Impression] Bilateral pneumonia. - [Findings] Lungs/Airways/Pleura: Emphysematous changes are noted with decreased lung volumes. [Impression] Lung volumes increased in size.</p> <p>Negation error examples: - [Findings] There is evidence of emphysema [Impression] No evidence of emphysema. - [Findings] Appendicitis is not seen [Impression] Appendicitis is seen.</p> <p>Most reports are transcribed by the automatic speech recognition (ASR) system and may result in transcription errors with words that might sound similar to a medical term. Some of these are single words and some may be multi-word terms. Examples: - 'chloral effusion' should be 'pleural effusion' - 'costal phrenic' should be 'costophrenic'</p> <p>{Clinical Conditions} - Aortic enlargement - Atelectasis - Cardiomegaly - Atherosclerotic Calcification - Clavicle fracture - Consolidation</p>	<ul style="list-style-type: none"> - Edema - Emphysema - Enlarged pulmonary artery - Interstitial lung disease (ILD) - Infiltration - Lung cavity - Lung cyst - Lung opacity - Nodule/Mass - Pulmonary fibrosis - Pneumothorax - Pleural thickening - Pleural effusion - Rib fracture - Other lesion - Lung tumor - Pneumonia - Tuberculosis - COPD <p>Synthetic Report Formatting Rules: - Words after a colon:' in the template and at the beginning of a new line should be capitalized, but not all capital letters. - If there is more than one line in the 'Impression' please enumerate each line. A single line in the 'Impression' should not be enumerated - Do not reorder the report – keep the template fields in the same order - Do not show the output wrapped in the triple quotes</p> <p>{Task 1 Instructions} Synthetic Report Generation - Enumerate the 'Patient ID: []' using 5-digits with zero padding: Patient ID: [00001] - Format the 'History []' with patient age, gender, and one or more clinical conditions or symptoms like this. Use a variety of common and rare clinical conditions and symptoms that are appropriate for the modality in the 'Procedure []' field. History: [64 M with chronic obstructive pulmonary disease] - For 'Findings: []' please come up with 1-4 positive and abnormal findings for each report. Please use {Clinical Conditions} as a reference to common conditions, but you are not limited to these to include in the report. - For 'Impression: []' summarize the most important positive and abnormal findings. Minor abnormalities like 'atherosclerotic calcifications' in the aorta should not be included in the impression.</p> <p>- For each Synthetic report, create a 'Synthetic Report With Errors' and inject one or more of the 'Common Errors' [interval change errors, left/right errors, negation errors, and gender discrepancies] or errors that you might see if you use ASR, like transcription errors with words that might sound similar to a medical term.</p> <p>- Please encapsulate the inserted errors in the 'Synthetic Report With Errors' with <e error="error description"> </e> markup and the corresponding correct text in the original 'Synthetic Report'. e.g., <e error="left/right error"> </e> , <e error="negation error"> </e> , <e error="transcription error"> </e> , <e error="interval change error"> </e></p> <p>Please generate 828 reports using {Task 1 Instructions} - Use a markdown table format: [Report Number, Synthetic Report, Synthetic Report With Errors, Error Type(s)]</p>
--	--

Figure 1: Prompts for GPT-4-0125-Preview used to generate 828 error-free synthetic reports and 828 synthetic reports with errors.

Table 1: Statistics of our constructed dataset. #Synthetic reports - the number of synthetic reports, #Reports from MIMIC - the number of synthetic reports and reports from the MIMIC-CXR Database.

	#Synthetic reports	#Reports from MIMIC
Total reports	1,656	614
Error-free reports	828	307
Reports with errors	828	307
Negation errors	299	99
Left/right errors	233	93
Interval change errors	62	91
Transcription errors	489	189
Training set	1,316	500
Test set	340	114

left/right, interval change, and transcription errors (Supplementary S1 and Supplementary Table 1).

In total, 828 pairs of synthetic radiology reports were obtained, with each pair comprising an error-free report and a report containing errors. During the proofreading process, the error-free report and the report containing errors were proofread independently to ensure an unbiased evaluation.

The second part of the dataset consisted of 307 reports from the MIMIC-CXR database and a set of corresponding reports with errors generated by GPT-4-0125-Preview (Figure 2). This process resulted in a total of 614 radiology reports: 307 error-free reports from the MIMIC-CXR database and 307 corresponding synthetic reports with errors.

For experimental evaluation, the dataset was split into training and test sets at an 8:2 ratio (Table 1), ensuring that each pair of error-free and error-containing reports remained in the same set.

2.2 Inter-Annotator Agreement Analysis

The Cohen kappa coefficient was used to evaluate the Inter-Annotator Agreement (IAA) of synthetic reports.

2.3 Model Development and Configurations

In this study, quantized low-rank adapters (QLoRA) [29] were used to fine-tune the Llama-3 models (i.e., Llama-3-8B-Instruct and Llama-3-70B-Instruct). Llama-3-8B-Instruct and Llama-3-70B-Instruct were refined on the training set and the test set was reserved for model evaluation. For comparison, we used GPT-4-1106-Preview and BiomedBERT as baseline models, with BiomedBERT fine-tuned on the same training set. The effectiveness of the models in detecting errors was measured via precision, recall, and F1-score metrics. The overall performance was assessed by the macro average F1 score across the four types of errors (computing resources can be found in Supplementary S2).

For GPT-4-1106-Preview, the API provided by Azure was accessed¹. Bootstrap analyses were performed using 100 bootstrap samples to estimate the distribution of the macro-F1 score, and 95% confidence intervals (CIs) were reported. In each bootstrap iteration, n reports were sampled from the test set with replacement. Additionally, paired-sample t-tests were used to compare model predictions across paired observations and assess statistical significance.

¹<https://azure.microsoft.com/en-us/blog/introducing-gpt4-in-azure-openai-service>

<p>You are a radiologist assistant helping audit radiology reports.</p> <p>Radiology reports can have a variety of errors and issues. 'Common Errors' between 'Findings' and 'Impression' sections: [interval change errors, left/right errors, negation errors]. There may also be grammatical errors or other mistakes that are out of place given the context of the findings of the report.</p> <p>Left right error examples:</p> <ul style="list-style-type: none"> - [Findings] Possible right upper lobe consolidation. [Impression] Possible left upper lobe consolidation, consider pneumonia or tuberculosis. - [Findings] Possible rib fracture on the right. [Impression] Possible left-sided rib fracture. <p>Interval change error examples:</p> <ul style="list-style-type: none"> - [Findings] Lungs/Airways/Pleura: Unilateral lower lobe consolidation, consistent with pneumonia. [Impression] Bilateral pneumonia. - [Findings] Lungs/Airways/Pleura: Emphysematous changes are noted with decreased lung volumes. [Impression] Lung volumes increased in size. <p>Negation error examples:</p> <ul style="list-style-type: none"> - [Findings] There is evidence of emphysema [Impression] No evidence of emphysema - [Findings] Appendicitis is not seen [Impression] Appendicitis is seen. <p>Most reports are transcribed by the automatic speech recognition (ASR) system and may result in transcription errors with words that might sound similar to a medical term. Some of these are single words and some may be multi-word terms.</p> <p>Examples:</p> <ul style="list-style-type: none"> - 'chloral effusion' should be 'pleural effusion' - 'costal phrenic' should be 'costophrenic' <p>{Clinical Conditions}</p> <ul style="list-style-type: none"> - Aortic enlargement - Atelectasis - Cardiomegaly - Atherosclerotic Calcification - Clavicle fracture - Consolidation - Edema 	<ul style="list-style-type: none"> - Emphysema - Enlarged pulmonary artery - Interstitial lung disease (ILD) - Infiltration - Lung cavity - Lung cyst - Lung opacity - Nodule/Mass - Pulmonary fibrosis - Pneumothorax - Pleural thickening - Pleural effusion - Rib fracture - Other lesion - Lung tumor - Pneumonia - Tuberculosis - COPD <p>Given this radiology report:</p> <p>Patient ID: s50414267 EXAMINATION: CHEST (PA AND LAT) INDICATION: ___F with new onset ascites // eval for infection TECHNIQUE: Chest PA and lateral COMPARISON: None. FINDINGS: There is no focal consolidation, pleural effusion or pneumothorax. Bilateral nodular opacities that most likely represent nipple shadows. The cardiomeastinal silhouette is normal. Clips project over the left lung, potentially within the breast. The imaged upper abdomen is unremarkable. Chronic deformity of the posterior left sixth and seventh ribs are noted. IMPRESSION: No acute cardiopulmonary process.</p> <p>Please encapsulate the inserted errors in the 'Synthetic Report With Errors' with <e error="error description"> </e> markup and the corresponding correct text in the original 'Synthetic Report'.</p> <p>e.g., <e error="left/right error"> </e> , <e error="negation error"> </e> , <e error="transcription error"> </e> , <e error="interval change error"> </e></p>
--	--

Figure 2: Prompts for GPT-4-0125-Preview utilized to generate synthetic radiology reports using reports from the MIMIC-CXR Database. The bold text indicates the original reports from the MIMIC-CXR database that were used to create these synthetic reports with errors.

<p>USER: You are a medical assistant. Please classify the input report and respond in JSON format {'Classification': 'Negation error, Left/Right error, Interval Change error, Transcription error, or No error'}. Note that the input report may belong to multiple errors. ASSISTANT: Sure! Please give the input report. USER: INPUT_REPORT</p>
<p>a. Prompts for zero-shot prompting.</p>
<p>USER: Here is an example of Example_Label. ASSISTANT: Example_Text USER: Please classify the input report and respond in JSON format {'Classification': 'Negation error, Left/Right error, Interval Change error, Transcription error, or No error'}. Note that the input report may belong to multiple errors. ASSISTANT: Sure! Please give the input report. USER: INPUT_REPORT</p>
<p>b. Prompts for one-shot prompting.</p>
<p>USER: Here is an example of Transcription errors. ASSISTANT: Example_Tran USER: Here is an example of Interval Change errors. ASSISTANT: Example_Int USER: Here is an example of Left/Right errors. ASSISTANT: Example_LR USER: Here is an example of Negation errors. ASSISTANT: Example_Neg USER: Please classify the input report and respond in JSON format {'Classification': 'Negation error, Left/Right error, Interval Change error, Transcription error, or No error'}. Note that the input report may belong to multiple errors. ASSISTANT: Sure! Please give the input report. USER: INPUT_REPORT</p>
<p>c. Prompts for four-shot prompting.</p>

Figure 3: Example prompt designs. (a) A zero-shot prompt. (b) A one-shot prompt. (c) A four-shot prompt. INPUT_REPORT - an input report from the test set. Example_Text - an example report from the training set, Example_Label - the label of the example report, Example_Tran - an example report containing a transcription error from the training set, Example_Int - an example report containing an interval change error, Example_LR - an example report containing a left/right error, Example_Neg - an example report containing a negation error.

2.4 Model Scale

In this study, two versions of Llama-3 were explored: Llama-3-8B-Instruct and Llama-3-70B-Instruct. Both were fine-tuned with a learning rate of 3×10^{-4} , a batch size of 1, a maximum sequence length of 512, and 3 training epochs. BiomedBERT was fine-tuned with a learning rate of 3×10^{-5} , a batch size of 4, a maximum sequence length of 512, and 3 training epochs. For inference, Llama-3-8B-Instruct, Llama-3-70B-Instruct, GPT-4-1106-Preview, and BiomedBERT were all inferred using a batch size of 1.

Prompt Designs

In this study, three strategies were employed: zero-shot, one-shot, and four-shot prompting (Figure 3). The zero-shot prompt design aims to detect errors without providing task-specific examples (Figure 3a). For the one-shot prompting strategy, a single radiology report was selected from the training set known to contain errors (Figure 3b). In the four-shot prompting strategy, we chose four distinct reports, each illustrating a different type of error (Figure 3c).

To further refine this approach, four strategies were explored for selecting example reports in the one-shot and four-shot prompting strategies: one-shot random, one-shot specified, four-shot random, and four-shot specified (Supplementary S3).

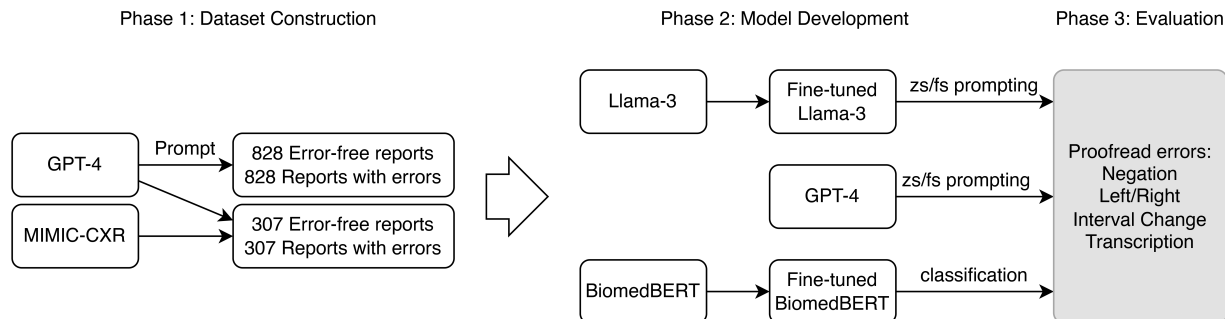


Figure 4: The overall workflow of Reportedly LLMs. A dataset was constructed by combining synthetic radiology reports with a small subset of reports from the MIMIC-CXR database, LLMs such as Llama-3 and GPT-4 were refined using zero-shot or few-shot prompting strategies, and the models’ performance on the constructed dataset was evaluated. zs - zero-shot, fs - few-shot.

2.5 Real-world Data Collection and Inference

The use of GPT-4-1106-Preview and the fine-tuned Llama-3-70B-Instruct for detecting errors in real-world radiology reports [30] was also explored. The dataset consisted of 122,025 thoracoabdominal chest X-ray reports from heart failure patients treated at New York-Presbyterian/Weill Cornell Medical Center (Supplementary S4). A total of 55,339 deidentified real-world radiology reports from this dataset were randomly collected and analyzed using GPT-4-1106-Preview and the fine-tuned Llama-3-70B-Instruct, with the aim of detecting errors and improving the accuracy and reliability of the radiology reports. A voting mechanism in which the two models independently detected errors in each of the 55,339 reports was employed to leverage the strengths of both models, increasing the likelihood of accurate error detection. The voting process identified 606 reports with errors, with both models detecting a specific type of error in these reports.

A power calculation was performed as follows: With 200 reports, a one-sample proportion test can achieve 81.3% power to detect the difference between the alternative hypothesis that the radiologist-confirmed error detection accuracy rate is 0.5 versus the null hypothesis that the radiologist-confirmed error detection accuracy rate is 0.4, at a type I error rate of 0.05.

3 Results

3.1 Technical Validation of Synthetic Data

An overview of this study is shown in Figure 4, and the code is available on GitHub². To evaluate the quality of the synthetic reports, 198 reports were selected, with each containing a single, specific error. These synthetic reports were generated via the GPT-4-0125-Preview following the methodology outlined in Figure 1. Each synthetic report, along with its error, was reviewed by a board-certified radiologist (G.K., 5 years of experience) and a radiology resident (B.C.) to determine whether the error type generated by GPT-4-0125-Preview was accurate. The error type was assigned when both experts reached a consensus.

In addition, the accuracy of the assigned error type for the synthetic reports with errors was calculated. Accuracy was defined as both experts reaching a consensus on the error type generated by GPT-4-0125-Preview, which was manually verified using the Doccano annotation tool³. Transcription errors were accurately introduced in 83% of the labeled reports (58/70). Left/right errors were the most accurately introduced errors, appearing in 95% of the intended reports (63/66). Negation errors were introduced in 63% of the labeled

²<https://github.com/bionlplab/llm4proofreading>

³<https://github.com/doccano/doccano>

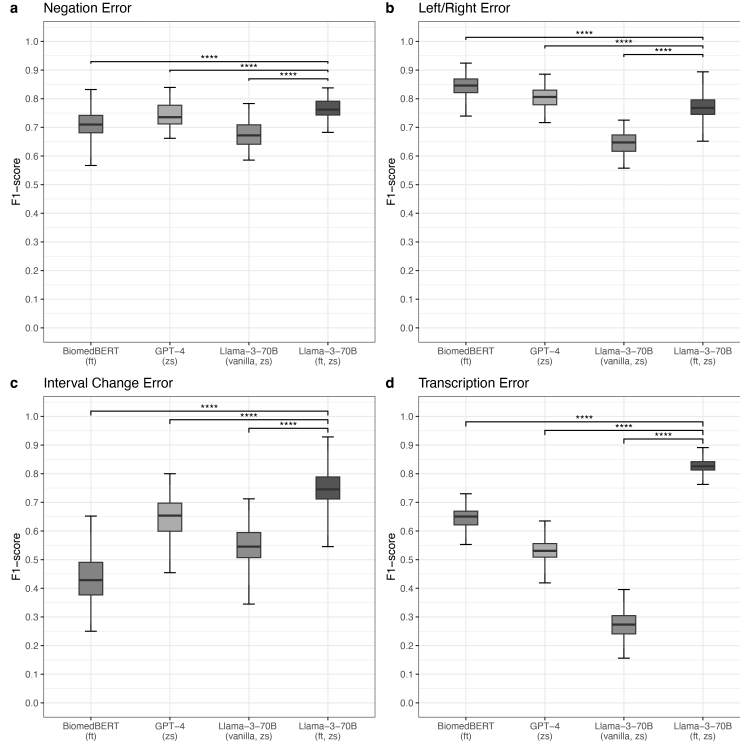


Figure 5: F1 scores of different models. (a) Negation error, (b) left/right error, (c) interval change error, (d) transcription error. BiomedBERT - BiomedBERT-base-uncased-abstract, GPT-4 - GPT-4-1106-Preview, Llama-3-70B - Llama-3-70B-Instruct, ft - fine-tuned, zs - zero-shot prompting. Significance levels: * - $p < 0.05$; ** - $p < 0.01$; *** - $p < 0.001$; **** - $p < 0.0001$; ns - Not significant. The error bars are 95% CIs.

reports (30/48), with most inaccuracies being due to omissions in the impressions rather than contradictions. Interval change errors that did not fall into either subcategory were introduced in 57% (8/14) of the intended reports. Reports with transcription errors had an average length of 56 words, whereas those with interval change, negation, and left/right errors had average lengths of 55, 57, and 58 words, respectively. There was no evidence of a difference between label accuracy and average report length by error category ($p > 0.05$).

3.2 Inter-Annotator Agreement

IAA was evaluated using the Cohen kappa coefficient on the basis of the reviews of the two experts, resulting in a value of 0.734.

3.3 Model Performance of Different LLMs in Error Detection

First, the performance of different models in detecting errors was compared within radiology reports (Figure 5 and Table 2). The evaluated models included BiomedBERT (fine-tuned), GPT-4-1106-Preview (zero-shot), Llama-3-70B-Instruct (vanilla, zero-shot), and Llama-3-70B-Instruct (fine-tuned, zero-shot).

The fine-tuned Llama-3-70B-Instruct (zero-shot) achieved the highest F1 scores across all the metrics, with a score of 0.769 (95% CI, 0.757-0.771) for detecting negation errors, 0.772 (95% CI, 0.762-0.780) for detecting left/right errors, 0.750 (95% CI, 0.736-0.763) for detecting interval change errors, and 0.828 (95% CI, 0.822-0.832) for detecting transcription errors. The overall macro-F1 score of 0.780 indicated that fine-tuning significantly enhances the model's performance in specialized tasks (Supplementary S5).

Table 2: Performance metrics of different models across error types. ft - fine-tuned, zs - zero-shot prompting.

Model	Error Type	Precision	Recall	F1
Llama-3-70B-Instruct (ft, zs)	Negation	0.873	0.688	0.769
	Left/Right	0.830	0.721	0.772
	Interval Change	0.913	0.636	0.750
	Transcription	0.914	0.757	0.828
	Macro F1	-	-	0.780
BiomedBERT (ft)	Negation	0.920	0.575	0.708
	Left/Right	0.891	0.803	0.845
	Interval Change	0.714	0.303	0.426
	Transcription	0.841	0.529	0.649
	Macro F1	-	-	0.657
GPT-4-1106-Preview (zs)	Negation	0.732	0.750	0.741
	Left/Right	0.765	0.852	0.806
	Interval Change	0.656	0.636	0.646
	Transcription	0.885	0.386	0.537
	Macro F1	-	-	0.683
Llama-3-70B-Instruct (vanilla, zs)	Negation	0.797	0.588	0.676
	Left/Right	0.514	0.885	0.651
	Interval Change	0.500	0.606	0.548
	Transcription	0.727	0.171	0.277
	Macro F1	-	-	0.538

3.4 Impact of the Parameter Scale on Model Performance

Figure 6 illustrates the impact of different model parameter scales on Llama-3. After fine-tuning, Llama-3-8B-Instruct showed strong performance in negation error detection, with an F1 score of 0.803 (95% CI, 0.798-0.813), highlighting its effectiveness in this specific task. However, it had worse performance in detecting interval change errors, with an F1 score of 0.646 (95% CI, 0.622-0.654), indicating a need for improvement in capturing these errors. On the other hand, Llama-3-70B-Instruct excelled in detecting interval changes and transcription errors, achieving F1 scores of 0.750 (95% CI, 0.736-0.762) and 0.828 (95% CI, 0.823-0.832), highlighting its ability to understand and track temporal variations while maintaining high accuracy in transcription error detection. Additionally, it had robust left/right error detection with an F1 score of 0.772 (95% CI, 0.766-0.782), indicating its good performance in spatial orientation tasks. Furthermore, Llama-3-70B-Instruct achieved a higher overall macro-F1 score of 0.780 than did Llama-3-8B-Instruct (0.749), reflecting its balanced and comprehensive performance across multiple tasks.

3.5 Impact of Different Prompting Strategies on Model Performance

Figure 7 shows the F1 scores of the fine-tuned Llama-3-70B-Instruct under different prompting strategies: one-shot random, one-shot specified, four-shot random, and four-shot specified. “Random” and “specified” refer to the selection of the input radiology report (i.e., INPUT_REPORT) in Figure 3. Details can be found in Supplementary Table 2 and Table 3.

Under one-shot prompting, Llama-3-70B-Instruct (specified) obtained F1 scores of 0.736 (95% CI, 0.736-

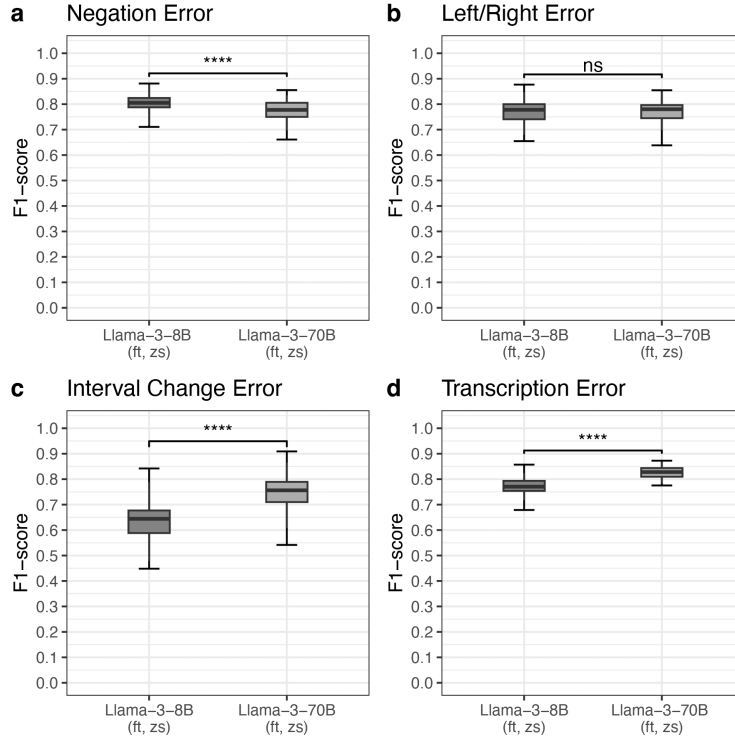


Figure 6: F1 scores for different model parameter scales. (a) Negation error, (b) left/right error, (c) interval change error, (d) transcription error. Llama-3-8B - Llama-3-8B-Instruct, Llama-3-70B - Llama-3-70B-Instruct, ft - fine-tuned, zs - zero-shot prompting. Significance levels: * - $p < 0.05$; ** - $p < 0.01$; *** - $p < 0.001$; **** - $p < 0.0001$; ns - Not significant. The error bars are 95% CIs.

0.752) for detecting negation errors, 0.672 (95% CI, 0.666-0.747) for detecting left/right errors, 0.549 (95% CI, 0.531-0.565) for detecting interval change errors, and 0.722 (95% CI, 0.719-0.730) for detecting transcription errors. In comparison, Llama-3-70B-Instruct (random) achieved F1 scores of 0.688 (95% CI, 0.683-0.701) for detecting negation errors, 0.754 (95% CI, 0.747-0.762) for detecting left/right errors, 0.642 (95% CI, 0.618-0.649) for detecting interval change errors, and 0.832 (95% CI, 0.825-0.835) for detecting transcription errors.

Under four-shot prompting, Llama-3-70B-Instruct (specified) achieved F1 scores of 0.646 (95% CI, 0.638-0.658) for detecting negation errors, 0.645 (95% CI, 0.641-0.662) for detecting left/right errors, 0.612 (95% CI, 0.585-0.623) for detecting interval change errors, and 0.780 (95% CI, 0.778-0.788) for detecting transcription errors. In contrast, Llama-3-70B-Instruct (random) achieved F1 scores of 0.579 (95% CI, 0.565-0.587) for detecting negation errors, 0.660 (95% CI, 0.655-0.675) for detecting left/right errors, 0.612 (95% CI, 0.593-0.624) for detecting interval change errors, and 0.784 (95% CI, 0.775-0.787) for detecting transcription errors.

3.6 Results in real-world scenarios

To further validate the accuracy of the models' detection, 200 reports (50 for each error type) were randomly selected from the 606 reports and reviewed by two board-certified radiologists (G.K., 5 years of experience; D.N., 1.5 years of experience). Upon confirmation by both radiologists, 99 out of 200 radiology reports were unanimously identified as containing the errors detected by the models, indicating an overall accuracy rate of 0.495 (95% CI: 0.424-0.566) in error detection (Figure 8a). Notably, there were considerable differences

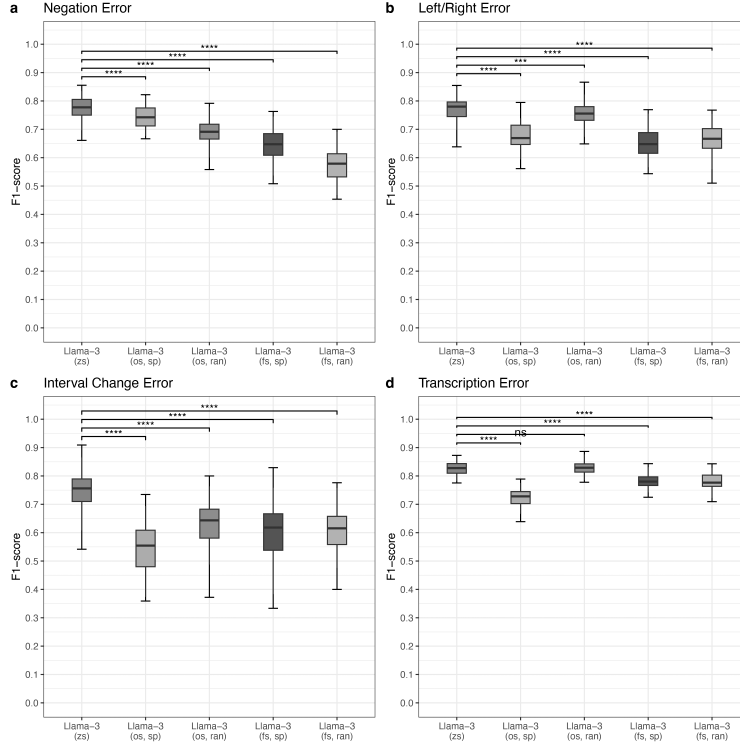


Figure 7: F1 scores of Llama-3-70B-Instruct under different prompting strategies. (a) Negation error, (b) left/right error, (c) interval change error, (d) transcription error. Llama-3 - fine-tuned Llama-3-70B-Instruct model, zs - zero-shot prompting, os - one-shot prompting, fs - four-shot prompting, sp - specified, ran - random. Significance levels: * - $p < 0.05$; ** - $p < 0.01$; *** - $p < 0.001$; **** - $p < 0.0001$; ns - Not significant. The error bars are 95% CIs.

($p < 0.05$) in the accuracy for each specific type of error (typical examples can be found in Supplementary Table 4). Additionally, cases where at least one of the two radiologists agreed with the errors detected by the models were analyzed (Figure 8b). Of the 200 reports with errors introduced, 163 were found to contain errors, resulting in an overall error detection accuracy rate of 0.815 (95% CI: 0.753-0.865). Details of each error can be found in Supplementary S6.

4 Discussion

This study provided evidence that LLMs can assist in detecting various types of errors, including negation, left/right, interval change, and transcription errors. The application of LLMs in medical proofreading may help reduce the occurrence of inaccuracies in radiology reports. However, their effectiveness depends on model selection, fine-tuning strategies, and prompt design. The analysis of the fine-tuned Llama-3-70B-Instruct under different prompting strategies revealed that zero-shot learning provides a reasonable degree of generalizability across all tasks. While few-shot learning can improve performance in specific tasks, such as transcription detection, its effectiveness is highly dependent on the relevance and specificity of the provided examples. These findings suggest that careful selection of examples in few-shot prompts can affect model performance but does not guarantee consistent improvements across all types of errors.

The experimental results demonstrated that the fine-tuned Llama-3-70B-Instruct achieves higher F1 scores than do baseline models such as BiomedBERT and GPT-4-1106-Preview. These findings indicate that fine-tuning enhances model performance in specialized tasks; however, the impact of fine-tuning may vary de-

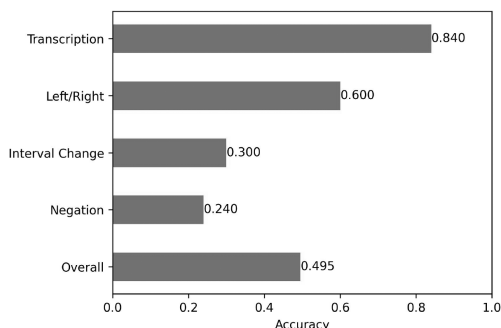
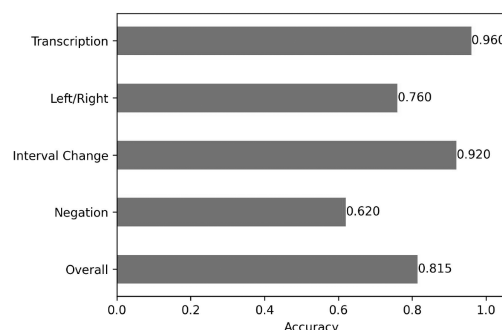
a Errors confirmed by both radiologists**b Errors confirmed by at least one radiologist**

Figure 8: Radiologist-confirmed accuracy of error detection across different categories in radiology reports. (a) Errors confirmed by both radiologists. (b) Errors confirmed by at least one radiologist.

pending on error complexity and the model’s generalization ability. While fine-tuning can improve performance, its ability to reduce radiologists’ cognitive load and enhance patient care requires further real-world validation.

Despite the promising performance, we recognize several limitations to this study. First, the fine-tuning process requires substantial computational resources and high-quality annotated radiology reports, which may pose feasibility concerns for some institutions. Indeed, the reliance on high-performance GPUs and high-quality annotated data for effective model fine-tuning and inference could limit the widespread adoption of these advanced LLMs in smaller clinical settings. Second, while this study focused on detecting errors in radiology reports, its generalizability to other medical documents or clinical notes remains uncertain. Although the performance of LLMs in real-world radiology report scenarios has been validated by radiologists, these models may still face unexpected challenges in diverse clinical environments. Third, another limitation is the potential for overfitting during the fine-tuning process. The models are specifically fine-tuned on a dataset tailored for radiology report proofreading, which may limit their adaptability to different types of errors or variations in report styles that are not covered in the training data. Finally, the errors in our constructed dataset were synthetic by design. While synthetic data have been praised for their use in addressing challenges related to data scarcity and privacy, they also raise concerns about bias [31]. In our study, we ensured that the synthetic data were generated from diverse and representative samples of real-world data to minimize such bias. We also validated synthetic errors by having radiologists assess their accuracy and reliability. However, synthetic errors may not fully capture the complexity of real-world errors in radiology reports. Future work could include a systematic evaluation of how bias introduced by synthetic errors affects model performance.

In conclusion, this study highlights the potential of fine-tuned LLMs in enhancing error detection within radiology reports, providing an efficient and accurate tool for medical proofreading. The findings highlight that fine-tuning is crucial for enabling the local deployment of LLMs while also demonstrating the importance of prompt design in optimizing performance for specific medical tasks.

Disclosures of conflicts of interest: No conflicting relationships exist for any author.

Acknowledgement: Supported by the National Science Foundation Faculty Early Career Development (CAREER) award number 2145640, the National Institute of Biomedical Imaging and Bioengineering (NIBIB) under grant number 75N920202D00021, the National Cancer Institute (NCI) under the grant num-

ber R01CA289249, and the Advanced Research Projects Agency for Health (ARPA-H).

References

- [1] P Grenier, D Valeyre, P Cluzel, M W Brauner, S Lenoir, and C Chastang. Chronic diffuse interstitial lung disease: diagnostic value of chest radiography and high-resolution CT. *Radiology*, 179(1):123–132, April 1991. ISSN 0033-8419,1527-1315. doi: 10.1148/radiology.179.1.2006262.
- [2] U Bick and H Lenzen. PACS: the silent revolution. *Eur. Radiol.*, 9(6):1152–1160, 1999. ISSN 0938-7994,1432-1084. doi: 10.1007/s003300050811.
- [3] John A Pezzullo, Glenn A Tung, Jeffrey M Rogg, Lawrence M Davis, Jeffrey M Brody, and William W Mayo-Smith. Voice recognition dictation: radiologist as transcriptionist. *J. Digit. Imaging*, 21(4):384–389, December 2008. ISSN 0897-1889,1618-727X. doi: 10.1007/s10278-007-9039-2.
- [4] Chian A Chang, Rodney Strahan, and Damien Jolley. Non-clinical errors using voice recognition dictation software for radiology reports: a retrospective audit. *J. Digit. Imaging*, 24(4):724–728, August 2011. ISSN 0897-1889,1618-727X. doi: 10.1007/s10278-010-9344-z.
- [5] C Matthew Hawkins, Seth Hall, Bin Zhang, and Alexander J Towbin. Creation and implementation of department-wide structured reports: an analysis of the impact on error rate in radiology reports. *J. Digit. Imaging*, 27(5):581–587, October 2014. ISSN 1618-727X,0897-1889. doi: 10.1007/s10278-014-9699-7.
- [6] Matthew J Minn, Arash R Zandieh, and Ross W Filice. Improving radiology report quality by rapidly notifying radiologist of report errors. *J. Digit. Imaging*, 28(4):492–498, August 2015. ISSN 1618-727X,0897-1889. doi: 10.1007/s10278-015-9781-9.
- [7] Michael A Bruno, Eric A Walker, and Hani H Abujudeh. Understanding and confronting our mistakes: The epidemiology of error in radiology and strategies for error reduction. *Radiographics*, 35(6):1668–1676, October 2015. ISSN 0271-5333,1527-1323. doi: 10.1148/rg.2015150023.
- [8] Stephen Waite, Jinel Scott, Brian Gale, Travis Fuchs, Srinivas Kolla, and Deborah Reede. Interpretive error in radiology. *AJR Am. J. Roentgenol.*, 208(4):739–749, April 2017. ISSN 0361-803X,1546-3141. doi: 10.2214/AJR.16.16963.
- [9] Stephen Waite, Jinel Moore Scott, Alan Legasto, Srinivas Kolla, Brian Gale, and Elizabeth A Krupinski. Systemic error in radiology. *AJR Am. J. Roentgenol.*, 209(3):629–639, September 2017. ISSN 0361-803X,1546-3141. doi: 10.2214/AJR.16.17719.
- [10] Bibb Allen, Mythreyi Chatfield, Judy Burleson, and William T Thorwarth. Improving diagnosis in health care: perspectives from the american college of radiology. *Diagnosis (Berl)*, 4(3):113–124, 26 September 2017. ISSN 2194-8011,2194-802X. doi: 10.1515/dx-2017-0020.
- [11] Lawrence H Schwartz, David M Panicek, Alexandra R Berk, Yuelin Li, and Hedvig Hricak. Improving communication of diagnostic radiology findings through structured reporting. *Radiology*, 260(1):174–181, July 2011. ISSN 0033-8419,1527-1315. doi: 10.1148/radiol.11101913.
- [12] David B Larson, Alex J Towbin, Rebecca M Pryor, and Lane F Donnelly. Improving consistency in radiology reporting through the use of department-wide standardized structured reporting. *Radiology*, 267(1):240–250, April 2013. ISSN 0033-8419,1527-1315. doi: 10.1148/radiol.12121502.

- [13] Dhakshinamoorthy Ganeshan, Phuong-Anh Thi Duong, Linda Probyn, Leon Lenchik, Tatum A McArthur, Michele Retrouvey, Emily H Ghobadi, Stephane L Desouches, David Pastel, and Isaac R Francis. Structured reporting in radiology. *Acad. Radiol.*, 25(1):66–73, January 2018. ISSN 1076-6332,1878-4046. doi: 10.1016/j.acra.2017.08.005.
- [14] J Martijn Nobel, Koos van Geel, and Simon G F Robben. Structured reporting in radiology: a systematic review to explore its potential. *Eur. Radiol.*, 32(4):2837–2854, April 2022. ISSN 0938-7994,1432-1084. doi: 10.1007/s00330-021-08327-5.
- [15] John Zech, Jessica Forde, Joseph J Titano, Deepak Kaji, Anthony Costa, and Eric Karl Oermann. Detecting insertion, substitution, and deletion errors in radiology reports using neural sequence-to-sequence models. *Ann. Transl. Med.*, 7(11):233, June 2019. ISSN 2305-5839,2305-5847. doi: 10.21037/atm.2018.08.11.
- [16] Seppo Enarvi, Marilisa Amoia, Miguel Del-Agua Teba, Brian Delaney, Frank Diehl, Stefan Hahn, Kristina Harris, Liam McGrath, Yue Pan, Joel Pinto, Luca Rubini, Miguel Ruiz, Gagandeep Singh, Fabian Stemmer, Weiyi Sun, Paul Vozila, Thomas Lin, and Ranjani Ramamurthy. Generating medical reports from patient-doctor conversations using sequence-to-sequence models. In *Proceedings of the First Workshop on Natural Language Processing for Medical Conversations*, Stroudsburg, PA, USA, 2020. Association for Computational Linguistics. doi: 10.18653/v1/2020.nlpmc-1.4.
- [17] Gunvant R Chaudhari, Tengxiao Liu, Timothy L Chen, Gabby B Joseph, Maya Vella, Yoo Jin Lee, Thienkhai H Vu, Youngho Seo, Andreas M Rauschecker, Charles E McCulloch, and Jae Ho Sohn. Application of a domain-specific BERT for detection of speech recognition errors in radiology reports. *Radiol. Artif. Intell.*, 4(4):e210185, 25 July 2022. ISSN 2638-6100. doi: 10.1148/ryai.210185.
- [18] Dabin Min, Kaeun Kim, Jong Hyuk Lee, Yisak Kim, and Chang Min Park. RRED : A radiology report error detector based on deep learning framework. In *Proceedings of the 4th Clinical Natural Language Processing Workshop*, Stroudsburg, PA, USA, 2022. Association for Computational Linguistics. doi: 10.18653/v1/2022.clinicalnlp-1.5.
- [19] Xiaoyan Cai, Sen Liu, Junwei Han, Libin Yang, Zhenguo Liu, and Tianming Liu. ChestXRyBERT: A pretrained language model for chest radiology report summarization. *IEEE Trans. Multimedia*, 25: 845–855, 2023. ISSN 1520-9210,1941-0077. doi: 10.1109/tmm.2021.3132724.
- [20] Daiki Nishigaki, Yuki Suzuki, Tomohiro Wataya, Kosuke Kita, Kazuki Yamagata, Junya Sato, Shoji Kido, and Noriyuki Tomiyama. BERT-based transfer learning in sentence-level anatomic classification of free-text radiology reports. *Radiol. Artif. Intell.*, 5(2):e220097, 15 March 2023. ISSN 2638-6100. doi: 10.1148/ryai.220097.
- [21] Jordan Hoffmann, Sebastian Borgeaud, Arthur Mensch, Elena Buchatskaya, Trevor Cai, Eliza Rutherford, Diego de Las Casas, Lisa Anne Hendricks, Johannes Welbl, Aidan Clark, Tom Hennigan, Eric Noland, Katie Millican, George van den Driessche, Bogdan Damoc, Aurelia Guy, Simon Osindero, Karen Simonyan, Erich Elsen, Jack W Rae, Oriol Vinyals, and Laurent Sifre. Training compute-optimal large language models. *arXiv [cs.CL]*, 29 March 2022. doi: 10.5555/3600270.3602446.
- [22] Jason Wei, Xuezhi Wang, Dale Schuurmans, Maarten Bosma, Brian Ichter, Fei Xia, Ed Chi, Quoc Le, and Denny Zhou. Chain-of-thought prompting elicits reasoning in large language models. In S Koyejo, S Mohamed, A Agarwal, D Belgrave, K Cho, and A Oh, editors, *Advances in Neural Information Processing Systems*, volume 35, pages 24824–24837. Curran Associates, Inc., 27 January 2022.

- [23] Tugba Akinci D’Antonoli, Arnaldo Stanzione, Christian Bluethgen, Federica Vernuccio, Lorenzo Ugga, Michail E Klontzas, Renato Cuocolo, Roberto Cannella, and Burak Koçak. Large language models in radiology: fundamentals, applications, ethical considerations, risks, and future directions. *Diagn. Interv. Radiol.*, 30(2):80–90, 6 March 2024. ISSN 1305-3612,1305-3825. doi: 10.4274/dir.2023.232417.
- [24] Lisa C Adams, Daniel Truhn, Felix Busch, Avan Kader, Stefan M Niehues, Marcus R Makowski, and Keno K Bressemer. Leveraging GPT-4 for post hoc transformation of free-text radiology reports into structured reporting: A multilingual feasibility study. *Radiology*, 307(4):e230725, May 2023. ISSN 1527-1315,0033-8419. doi: 10.1148/radiol.230725.
- [25] Arya Rao, John Kim, Meghana Kamineni, Michael Pang, Winston Lie, Keith J Dreyer, and Marc D Succi. Evaluating GPT as an adjunct for radiologic decision making: GPT-4 versus GPT-3.5 in a breast imaging pilot. *J. Am. Coll. Radiol.*, 20(10):990–997, October 2023. ISSN 1558-349X,1546-1440. doi: 10.1016/j.jacr.2023.05.003.
- [26] Roman Johannes Gertz, Alexander Christian Bunck, Simon Lennartz, Thomas Dratsch, Andra-Iza Iuga, David Maintz, and Jonathan Kottlors. GPT-4 for automated determination of radiological study and protocol based on radiology request forms: A feasibility study. *Radiology*, 307(5):e230877, June 2023. ISSN 1527-1315,0033-8419. doi: 10.1148/radiol.230877.
- [27] Roman Johannes Gertz, Thomas Dratsch, Alexander Christian Bunck, Simon Lennartz, Andra-Iza Iuga, Martin Gunnar Hellmich, Thorsten Persigehl, Lenhard Pennig, Carsten Herbert Gietzen, Philipp Fervers, David Maintz, Robert Hahnfeldt, and Jonathan Kottlors. Potential of GPT-4 for detecting errors in radiology reports: Implications for reporting accuracy. *Radiology*, 311(1):e232714, April 2024. ISSN 1527-1315,0033-8419. doi: 10.1148/radiol.232714.
- [28] Reuben A Schmidt, Jarrel C Y Seah, Ke Cao, Lincoln Lim, Wei Lim, and Justin Yeung. Generative large language models for detection of speech recognition errors in radiology reports. *Radiol. Artif. Intell.*, 6(2):e230205, March 2024. ISSN 2638-6100. doi: 10.1148/ryai.230205.
- [29] Tim Dettmers, Artidoro Pagnoni, Ari Holtzman, and Luke Zettlemoyer. QLoRA: Efficient finetuning of quantized LLMs. *Neural Inf Process Syst*, abs/2305.14314:10088–10115, 23 May 2023. doi: 10.48550/arXiv.2305.14314.
- [30] Mohit Pandey, Zhuoran Xu, Evan Sholle, Gabriel Maliakal, Gurpreet Singh, Zahra Fatima, Daria Larine, Benjamin C Lee, Jing Wang, Alexander R van Rosendael, Lohendran Baskaran, Leslee J Shaw, James K Min, and Subhi J Al’Aref. Extraction of radiographic findings from unstructured thoracoabdominal computed tomography reports using convolutional neural network based natural language processing. *PLoS One*, 15(7):e0236827, 30 July 2020. ISSN 1932-6203. doi: 10.1371/journal.pone.0236827.
- [31] Mauro Giuffrè and Dennis L Shung. Harnessing the power of synthetic data in healthcare: innovation, application, and privacy. *NPJ Digit. Med.*, 6(1):186, 9 October 2023. ISSN 2398-6352. doi: 10.1038/s41746-023-00927-3.

Supplementary materials

S1 Descriptions of the four error types

- Negation errors occur when negative phrases are incorrectly used or omitted, leading to a complete reversal of the intended meaning. For example, the correct statement “no signs of pneumonia” in the findings section might be incorrectly rewritten as “signs of pneumonia” in the impression section.
- Left/right errors involve the incorrect labeling of anatomical sides, such as mistakenly describing a condition on the left lung when it is actually on the right.
- Interval change errors refer to any modification within the report that alters key information or details, such as changes in measurement values or descriptions of findings that could lead to misinterpretation.
- Transcription errors simulate common mistakes made during the transcription of radiology reports, including typographical errors, misspellings, and incorrect medical terminology, which could lead to misunderstandings.

S2 Computing Resources

Experiments were conducted on two NVIDIA A100 GPUs with 80 GB of memory to ensure proper fine-tuning and inference of the LLMs. Dual A100 GPUs were used for inferring the Llama-3-70B-Instruct model and its fine-tuned version. For the fine-tuning and inference of Llama-3-8B-Instruct and BiomedBERT, a single A100 GPU was used.

S3 Descriptions of random and specified prompting strategies

The random prompting strategy involved selecting radiology reports randomly from the training set. In contrast, the specified strategy used a more deliberate selection, in which reports were empirically chosen from the training set on the basis of specific instructions. These strategies allowed evaluation of the impact of different prompting strategies on model performance.

S4 Descriptions of the real-world radiology reports

These patients with the ICD-9 Code 428 or the ICD-10 Code I50 who were admitted and discharged between January 2008 and July 2018 were included. For each report, only the findings and impression sections were used. The data were reviewed and deidentified in accordance with IRB protocols.

S5 Performance of the baseline models

After fine-tuning, BiomedBERT achieved moderate performance across the various metrics. It performed particularly well in detecting left/right error, with an F1 score of 0.845 (95% CI, 0.839-0.852), indicating its strong performance in spatial orientation tasks. However, it showed worse performance in detecting interval changes and transcription errors, with F1 scores of 0.426 (95% CI, 0.418-0.451) and 0.649 (95% CI, 0.640-0.654), respectively.

GPT-4-1106-Preview (zero-shot) demonstrated robust performance across various metrics. It excelled in detecting negation and interval change errors, with F1 scores of 0.741 (95% CI, 0.733 - 0.750) and 0.646 (95% CI, 0.628 - 0.657), respectively. However, its ability to detect transcription errors was only moderate, with an F1 score of 0.537 (95% CI, 0.524-0.540), indicating room for improvement in this area.

Llama-3-70B-Instruct (vanilla, zero-shot) outperformed the other models. It achieved an F1 score of 0.676 (95% CI, 0.666-0.684) for detecting negation errors and 0.651 (95% CI, 0.639-0.654) for detecting left/right errors, showing its limitations in zero-shot settings. The F1 scores for detecting interval change errors and transcription errors were relatively low, at 0.548 (95% CI, 0.536-0.562) and 0.277 (95% CI, 0.263-0.281),

indicating that additional training is needed to improve its performance in these areas.

S6 Performance of each error in real-world scenarios

Based on confirmation by both radiologists, the error detection accuracy rates for negation, interval changes, and left/right errors were 12/50 (24%), 15/50 (30%), and 30/50 (60%), respectively. Encouragingly, for transcription errors, the LLMs demonstrated strong error detection capabilities, achieving a radiologist-confirmed accuracy rate of 42/50 (84%).

Based on confirmation by at least one radiologist, the error detection accuracy rates for negation and left/right errors were 31/50 (62%) and 38/50 (76%), respectively. Notably, for interval changes and transcription errors, the radiologist-confirmed detection accuracy rates were 46/50 (92%) and 48/50 (96%), respectively.

Supplementary Table 1: Examples of radiology reports with errors.

Error type	Definition	Example
Negation	Negation errors occur when negative phrases are incorrectly used or omitted, leading to a complete reversal of the intended meaning.	Patient ID: 00033 History: 30 F with sharp left-sided chest pain, evaluate for pleural effusion TECHNIQUE: AP chest and abdomen radiograph. COMPARISON: Radiograph from one day prior. FINDINGS: Lines/tubes: None Mediastinum/Heart: The cardiomeastinal silhouette is unremarkable. Lungs/Airways/Pleura: Evidence of pleural effusion. Lung fields are clear. Bones/Soft Tissue: No acute osseous abnormalities. Upper abdomen: Unremarkable IMPRESSION: No pleural effusion noted.
Left/Right	Left/right errors involve the incorrect labeling of anatomical sides, such as describing a condition on the left lung when it is actually on the right.	Patient ID: 00014 History: 45 M with history of pneumothorax TECHNIQUE: AP chest and abdomen radiograph. COMPARISON: Radiograph from one day prior. FINDINGS: Lines/tubes: None Mediastinum/Heart: The cardiomeastinal silhouette is unremarkable. Lungs/Airways/Pleura: Small pneumothorax present on the right side. Bones/Soft Tissue: No acute osseous abnormalities. Upper abdomen: Unremarkable IMPRESSION: Small pneumothorax noted on the left side.
Interval Change	Interval change errors refer to any modification within the report that alters key information or details.	Patient ID: 00001 History: 60 F with chest pain and history of hypertension Technique: AP chest and abdomen radiograph. Standard protocol Comparison: Radiograph from two days prior. Findings: Lines/tubes: None Mediastinum/Heart: The cardiomeastinal silhouette is unremarkable. Lungs/Airways/Pleura: No focal opacities, pneumothorax or pleural effusion. Bones/Soft Tissue: No acute osseous abnormalities. Upper abdomen: Unremarkable IMPRESSION: 1. Enlargement of the cardiomeastinal silhouette, consistent with cardiomegaly.
Transcription	Transcription errors simulate common mistakes made during the transcription of radiology reports.	INDICATION: ___F with shortness of breath // Please evaluate for pneumonia, effusions, edema TECHNIQUE: PA and lateral views of the chest. COMPARISON: ____. FINDINGS: The lungs are clear without consolidation, effusion or edema. Biapical starring, worse on the right is again noted. The cardiomeastinal silhouette is within normal limits. No acute osseous abnormalities. IMPRESSION: No acute cardiopulmonary process.

Supplementary Table 2: The “specified” examples used for one-shot learning in the experiments.

Error type	Example
Left/Right	<p>Patient ID: 00002 History: 59 M with recent cough and weight loss, suspected lung tumor Technique: AP chest and abdomen radiograph. Comparison: Radiograph from two days prior. Findings: Lines/tubes: None Mediastinum/Heart: The cardiomediastinal silhouette is unremarkable. Lungs/Airways/Pleura: Mass in the left upper lobe, suggestive of a lung tumor. No pleural effusion. Bones/Soft Tissue: No acute osseous abnormalities. Upper abdomen: Unremarkable IMPRESSION: Mass in the right upper lobe, likely a lung tumor.</p>

Supplementary Table 3: The “specified” examples used for four-shot learning in the experiments.

Error type	Example
Negation	<p>Patient ID: 00033 History: 30 F with sharp left-sided chest pain, evaluate for pleural effusion TECHNIQUE: AP chest and abdomen radiograph. COMPARISON: Radiograph from one day prior. FINDINGS: Lines/tubes: None Mediastinum/Heart: The cardiomeastinal silhouette is unremarkable. Lungs/Airways/Pleura: Evidence of pleural effusion. Lung fields are clear. Bones/Soft Tissue: No acute osseous abnormalities. Upper abdomen: Unremarkable IMPRESSION: No pleural effusion noted.</p>
Left/Right	<p>Patient ID: 00014 History: 45 M with history of pneumothorax TECHNIQUE: AP chest and abdomen radiograph. COMPARISON: Radiograph from one day prior. FINDINGS: Lines/tubes: None Mediastinum/Heart: The cardiomeastinal silhouette is unremarkable. Lungs/Airways/Pleura: Small pneumothorax present on the right side. Bones/Soft Tissue: No acute osseous abnormalities. Upper abdomen: Unremarkable IMPRESSION: Small pneumothorax noted on the left side.</p>
Interval Change	<p>Patient ID: 00001 History: 60 F with chest pain and history of hypertension Technique: AP chest and abdomen radiograph. Standard protocol Comparison: Radiograph from two days prior. Findings: Lines/tubes: None Mediastinum/Heart: The cardiomeastinal silhouette is unremarkable. Lungs/Airways/Pleura: No focal opacities, pneumothorax or pleural effusion. Bones/Soft Tissue: No acute osseous abnormalities. Upper abdomen: Unremarkable IMPRESSION: 1. Enlargement of the cardiomeastinal silhouette, consistent with cardiomegaly.</p>
Transcription	<p>INDICATION: ___F with shortness of breath // Please evaluate for pneumonia, effusions, edema TECHNIQUE: PA and lateral views of the chest. COMPARISON: ----. FINDINGS: The lungs are clear without consolidation, effusion or edema. Biapical starring, worse on the right is again noted. The cardiomeastinal silhouette is within normal limits. No acute osseous abnormalities. IMPRESSION: No acute cardiopulmonary process.</p>

Supplementary Table 4: Typical examples identified by fine-tuned Llama-3-70B-Instruct and GPT-4-1106-Preview and verified by two physicians.

Error type	Example
Negation	<p>Clinical statement: Syncope. Technique: Single AP chest dated 04/03/2010 at 07:32. No prior films available for comparison. Findings: The overall heart size is within normal limits. The lungs are well expanded and clear. Impression: Cardiomegaly with atherosclerotic changes thoracic aorta.</p>
Left/Right	<p>Technique: PA and lateral views of the chest. Supine and upright views of the abdomen. Comparison: 7/24/2009 (chest). No prior abdominal radiographs for comparison. Findings: Chest: Minimal patchy opacity at the right lung base may reflect atelectasis or consolidation. There is no pleural effusion or pneumothorax. The cardiomeastinal silhouette remains enlarged. Abdomen: There is no pneumoperitoneum. No dilated bowel is seen. Air is seen in the colon. Impression: 1. Enlarged cardiomeastinal silhouette. 2. Minimal left basilar atelectasis or consolidation. 3. Nonobstructive bowel gas pattern.</p>
Interval Change	<p>Clinical Statement: Abnormal chest sounds. Technique: AP view of the chest. Comparison: January 21, 2010. Findings: Persistent near-complete opacification on the left hemithorax with associated leftward cardiomeastinal shift, compatible with volume loss, is unchanged since the prior study. The right lung remains clear. Metallic rods and screws transfix the thoracic spine. Impression: Since January 21, 2010: 1. Near-complete opacification of the left hemithorax with associated leftward cardiomeastinal shift compatible with volume loss, increased since the prior study. Evaluation for superimposed focal consolidation is limited.</p>
Transcription	<p>Technique: Portable AP chest radiograph. Comparison: June 1, 2010. Findings: The lungs are clear. No pleural effusion or pneumothorax is identified. The cardiomeastinal silhouette is within normal limits. Radiopaque densities project across the chest. Impression: 1. No acute cardiopulmonary disease. 2. Densities projecting over the chest may be related to patient's clothing, clinically correlate with repeat examination as clinically indicated.</p>